THE UNIVERSITY *of* EDINBURGH

# Edinburgh Research Explorer

## Simplicity beneath Complexity: Counting Molecular Electrons Reveals Transients and Kinetics of Photodissociation Reactions

# Simplicity beneath Complexity: Counting Molecular Electrons Reveals Transients and Kinetics of Photodissociation Reactions

Jennifer M. Ruddock,[a,b] Nikola Zotev,[c] Brian Stankus,[a] Haiwang Yong,[a] Darren Bellshaw,[c] Sébastien Boutet,[b] Thomas J. Lane,[b] Mengning Liang,[b] Sergio Carbajo,[b] Wenpeng Du,[a] Adam Kirrander,[c] Michael Minitti,*[b] and Peter M. Weber*[a]

**Abstract:** Time-resolved pump-probe gas phase X-ray scattering signals, extrapolated to zero momentum transfer, provide a measure of the number of electrons in a system, an effect that arises from the coherent addition of elastic scattering from the electrons. This allows for the identification of reactive transients and the determination of the chemical reaction kinetics without the need for extensive scattering simulations or complicated inversion of scattering data. We examine the photodissociation reaction of trimethyl amine, and identify two reaction paths upon excitation to the 3p state at 200 nm: a fast dissociation path out of the 3p state to the dimethyl amine radical (16.6±1.2%), and a slower dissociation via internal conversion to the 3s state (83.4±1.2%). The time constants for the two reactions are 640±130 fs and 74±6 ps, respectively. In addition, it is found that the transient dimethyl amine radical has a N-C bond length of 1.45±0.02 Å and a CNC bond angle of 118°±4°.

The identification and characterization of short-lived and reactive intermediates in chemical reaction sequences remains a challenging problem. The large number of photons produced by X-ray Free-Electron Lasers allow us to study gas-phase samples[1,2,3,4] and the ultrashort pulse duration makes it possible to investigate the structure of transients that are not accessible with other methods.[5] We use the Linac Coherent Light Source (LCLS) X-ray Free-Electron Laser at SLAC National Accelerator Laboratory to measure ultrafast X-ray scattering during the photodissociation reaction of the molecule trimethylamine (TMA) excited by 200 nm light. The experiment reveals the reaction kinetics of the dissociation of TMA to methyl and dimethylamine radicals, and uncovers the structure of the reactive and short-lived dimethyl amine radical transient.

While a full analysis of the X-ray scattering data is complicated, the reaction products and the kinetics can be identified from the X-ray scattering signal in the limit of vanishing momentum transfer vectors, $q \rightarrow 0$, i.e. at small scattering angles. This conceptually simple yet powerful analysis relies on the fact that coherent elastic scattering in the gas-phase is an intramolecular phenomenon. While the scattering from different electrons in each molecule adds coherently, the elastic scattering from *different* molecules, i.e. intermolecular scattering, adds incoherently. This is attributed to the random positions of the molecules in the gas and the large intermolecular distances compared to the X-ray wavelength.[6] At small angles, the elastic scattering is therefore proportional to the *square* of the number of electrons in one molecule. Consequently, as the molecules dissociate into smaller fragments there is a characteristic decrease of the scattering signal at small angles.

Amines are an important group of molecules, due to their use in fertilizers and biological processes. TMA is a prototypical tertiary amine, with accessible spectroscopic properties. It is known to dissociate into radical transients, which, being unstable, are difficult to study but are important in combustion, atmospheric chemistry, and enzymatic processes. In general, dissociation reactions can be difficult to study spectroscopically, as spectroscopic properties change between reactant and products.[7]

The electronic structure and photodissociation dynamics of TMA have previously been explored using photoionization spectroscopy and molecular beam techniques. Cardoza *et al.* found that optical excitation at 207.8 nm initially prepares the $3p_z$ state.[8] Internal conversion leads to the $3p_x$ and $3p_y$ states with a time constant 540±75 fs, and then to the 3s state with a time constant of 2.9±0.2 ps as shown in Figure 1.[9] At higher energy, reached by two-photon excitation with 400 nm, a slightly faster 3s internal conversion time constant of 2.0 ps was found.[8] Using time-of-flight photoionization with excitation at 193 nm, Forde *et al.*[10,11] found three dissociative channels: a dominant (72±9%) channel involving a sequential reaction to N-methylmethanimine (NMMA); a minor channel (27±9%) resulting in dimethylamine (DMA) and methyl ($CH_3$) radicals ejected with higher kinetic energy; and, possibly, a trace amount of a third channel involving a secondary dissociation of DMA resulting in $NC_2H_4$ and molecular hydrogen with low kinetic energy. In the dominant pathway, the initially excited TMA first dissociates to DMA and $CH_3$, and then DMA fragments to form NMMA and hydrogen atoms. Because the experiments by Forde *et al.* only identified the final reaction products they could not measure the time scales of the kinetic steps, nor confirm the electronic or geometrical structures of the DMA transients. The intermediate reaction steps and the nature of the transient species therefore remain largely unknown. The time-resolved X-ray scattering experiment reported here provides the missing rate constants of the dissociation paths. Within the time window of the experiment, up to 1 ns after the initial excitation, we found no signature of the secondary

[a] Department of Chemistry, Brown University
324 Brook St Providence, RI 02912 (USA)
*Professor Peter M. Weber
E-mail: peter_weber@brown.edu
[b] SLAC National Accelerator Laboratory
2575 Sandhill Rd Menlo Park, CA 94025 (USA)
*Michael Minitti
E-mail: minitti@slac.stanford.edu
[c] EaStCHEM, School of Chemistry, University of Edinburgh
David Brewster Road, Edinburgh EH9 3FJ (UK)

Supporting information for this article is given via a link at the end of the document.

dissociation of DMA to NMMA and hydrogen atoms, meaning that the DMA transient appears as a final reaction product.

Scattering signals were measured with the UV pump laser on and with the pump laser off, giving rise to scattering patterns $I_{on}(q,t)$ and $I_{off}(q)$, where $t$ is the delay time between the laser pump pulse and the X-ray probe pulse and $q$ is the amplitude of the momentum transfer vector. Details about the experiments are provided in the Supporting Information. It is convenient to express the pump-probe signal as a percent difference,

$$\%\Delta I(q,t) = 100 \frac{I_{on}(q,t) - I_{off}(q)}{I_{off}(q)}, \qquad \text{Eq. (1)}$$

in which poorly defined experimental parameters, such as background signals, pixel-to-pixel sensitivity variations of the detector, and gas pressure fluctuations cancel out. The percent difference signal is proportional to the excitation fraction, which is kept low to minimize unwanted multiphoton processes.
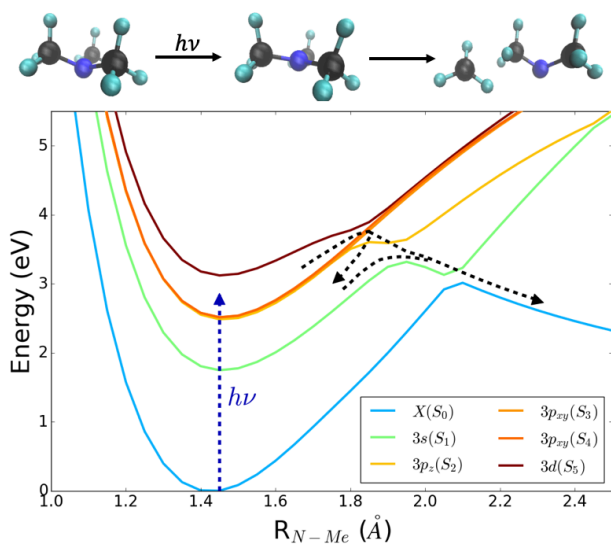


**Figure 1.** Reaction path of TMA upon UV excitation. (Top) Schematic of the dissociation of TMA upon UV excitation. (Bottom) The adiabatic potential energy curves calculated at the state-averaged CASSCF level (SA6-CAS(2,6)/6-31+G*) using the 3s optimized geometry, where a single N-Me distance was varied while all other coordinates were kept frozen. The states are labeled $\beta$ ($S\alpha$), where $\beta$ refers to the state character at the minimum energy geometry of the plot and $\alpha$ simply orders the adiabatic singlet states by energy. The blue dashed arrow indicates the excitation pulse. The black dashed arrows indicate the 3p → 3s internal conversion and the dissociative pathway.

The elastic scattering from a molecule is determined by its electron density distribution, [12] averaged over vibrational and rotational degrees of freedom. In pump-probe experiments the optical excitation might alter the electron density[13,14,15,16] and vibrational probability distributions,[4,5,15,17] and the laser and X-ray beam polarizations may cause anisotropies that combine with the rotational motions of the molecule to create alignment effects. The signals are furthermore averaged over the temporal profiles of the UV pump pulse and the X-ray probe pulse. To fully analyze pump-probe X-ray scattering patterns all those phenomena need to be considered. The complexity of such a complete analysis constitutes a bottleneck, although successful examples have been achieved.[18,19,20,21]

Beneath this complexity, however, lies the opportunity to extract valuable information about chemical reaction kinetics by considering the total electron counts of the molecular scatterers.

Polarization effects can be ignored as we only look at the isotropic scattering signal. Before dissociation, the scattering cross section in the limit of zero momentum transfer, i.e. $q \to 0$, is given by

$$\left(\frac{dI}{d\Omega}\right)(q \to 0) = \left(\frac{dI}{d\Omega}\right)_{Th} N^2, \qquad \text{Eq. (2)}$$

where $N$ is the number of electrons in a molecule, and $(dI/d\Omega)_{Th}$ is the Thomson differential scattering cross section,[6,15] with the square appearing due to the coherent addition of elastic scattering from different electrons within each molecule as discussed in the introduction. As the molecules in the sample dissociate and we end up with a gaseous mixture of fragment molecules $\alpha$, with the intermolecular distances large compared to the wavelength of the scattered X-ray radiation, the coherence of the waves scattered from different parts of the molecule is lost so that their scattering signals add up incoherently for all but the smallest values of $q$. Therefore, for experimentally accessible ranges of $q$, the scattering from different fragments becomes additive such that,

$$\left(\frac{dI}{d\Omega}\right)(q \to 0) = \left(\frac{dI}{d\Omega}\right)_{Th} \sum_\alpha N_\alpha^2, \qquad \text{Eq. (3)}$$

where $N = \sum_\alpha N_\alpha$ with $N_\alpha$ the number of electrons in the fragments, leading to the characteristic decrease in the small-angle scattering intensity. Of course, there is also the intermediate case, in which a molecule is in the process of dissociation, and an electron cannot be clearly associated with either fragment. However, presently we are interested a qualitative analysis made possible by Eqs. (2) and (3), noting that the fraction of molecules at intermediate separation is negligible compared to the fraction of the reactant and products at any given time.

With one nitrogen atom, three carbons and nine hydrogen atoms, TMA has 34 electrons. The scattering signal extrapolated to $q \to 0$ is therefore proportional to $34^2 = 1156$. The initial excitation to the 3p state and subsequent internal conversion to 3s changes the molecule's electron density distribution, and thus the shape of the scattering signal in $q$-space, but not the total electron count. Consequently, for $q \to 0$ the percent difference given by Eq. (1), considering the scattering signal from ground-state TMA and TMA in the excited 3s state, is expected to be zero. In contrast, for the two fragment molecules DMA and $CH_3$, the $q \to 0$ scattering signal is proportional to $25^2 + 9^2 = 706$. Therefore, if the reaction to DMA and $CH_3$ is complete, the $q \to 0$ percent difference signal is reduced compared to the unreacted molecule by $100(706 - 1156)/1156 = -38.9\%$. We emphasize that there are no instrumental parameters in this percent difference. In an experiment, the percentage is coupled with the overall excitation probability, which is independent of time delay and can therefore be separated in the analysis.
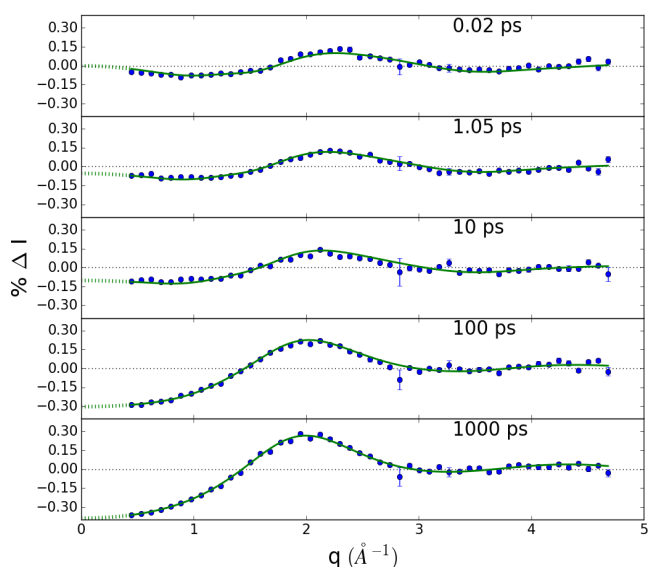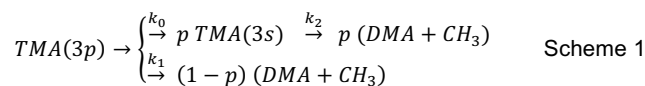
**Figure 2.** Experimental pump-probe X-ray scattering percent difference signals (blue dots) of TMA at select delay times as given. The signals are scaled by the experimentally determined percent excitation of 1.83%. The green solid lines are fits as described in the text, dashed lines are extrapolated for $q \to 0$. A dissociation reaction leads to a characteristic decrease of the signal at small values of $q$.

A selection of the pump-probe X-ray percent difference scattering curves, measured for $q$ in the range from 0.3 Å$^{-1}$ to 4.7 Å$^{-1}$, are shown in Figure 2. Even though the gas pressure was small (6 Torr) and the interaction length short (2.4 mm), the X-rays of LCLS are so bright that scattering patterns of excellent quality are obtained. Using a radiofrequency-based locking system,[22] the time delays between the UV pump pulses and the X-ray probe pulses were adjusted between -2 ps and 3 ns. For finer resolution in the time delays, the pump-probe timing techniques previously reported were used.[17] Due to the small interaction region and large translational energy of the dissociation fragments, the 3 ns time point was not viable for analysis.

The postulated reaction scheme includes a two-step decay via the lower 3s (S1) Rydberg state as well as the possibility of a direct reaction out of the 3p (S2/S3/S4) manifold,

$$TMA(3p) \to \begin{cases} \overset{k_0}{\to} p\,TMA(3s) \overset{k_2}{\to} p\,(DMA + CH_3) \\ \overset{k_1}{\to} (1-p)\,(DMA + CH_3) \end{cases} \quad \text{Scheme 1}$$

with rate constants $k_0$, $k_1$, and $k_2$, and a fraction $(1-p)$ of the excited molecules undergoing a single-step dissociation that has not previously been observed. The $k_0$ time constant is associated with internal conversion to 3s. Our experiment is blind to this process, but previous experiment determined the time constant $1/k_0$ to be 2.0 ps.[9] From the time sequence of scattering patterns, Figure 2, we infer that the observed reaction is complete at the 1 ns time point. This is apparent from the extrapolations to q→0 (green dotted lines), which show the low-q scattering decreases from 0 at small times to -0.389 at 1 ns, as expected. We can use this 1 ns pattern to determine the structure of the transient DMA radical, Figure 3. To calculate the percent difference scattering signal, we use the known structures of TMA[23] and the methyl radical.[24] Keeping the methyl C-H distances in DMA fixed and varying the C-N bond lengths and C-NC bond angle, we can fit the experimental pattern. The resulting N-C bond length is 1.45 ± 0.02 Å and the C-N-C bond angle is 118 ± 4°. The structure calculated at CAS(3,3)/6-311+G* level of theory has a bond length is 1.44 Å, and bond angle is 112°. We note that the nascent DMA radical might have substantial internal energy, which could result in a higher bond angle. The scattering signal of the electronically excited TMA species, given by the early time points before the reaction has significantly evolved, reflects both the changes in the electron density distribution upon electronic excitation and the high degree of vibrational excitation of the transients. A complete simulation of this pattern requires an in-depth quantum mechanical analysis that will be presented in the future.

With the scattering signals of the early and late time points as experimentally determined, the kinetics of the reaction can be obtained by fitting the time dependent scattering patterns (Figure 2) to Scheme 1 using the following equation:

$$\%\Delta I(q,t) = A_{TMA^*}(q)[(1-p)e^{-k_1 t} + pe^{-k_2 t}]$$

$$+ A_{DMA}(q)[1 - (1-p)e^{-k_1 t} - pe^{-k_2 t}] \quad \text{Eq. (6)}$$

$A_{TMA^*}(q)$ and $A_{DMA}(q)$ are the scattering signals arising from the electronically excited TMA$^*$ and the (DMA + CH$_3$) radical fragments, respectively. Eq. (6) is simplified for the case where $k_1 \gg k_2$, as appropriate for this reaction, and recognizes that the analysis does not distinguish between the initially excited 3p (S2/S3/S4) states and the 3s (S1) state reached by internal conversion. Both states have a planar geometry about the central nitrogen, and the effect of the diffuse Rydberg electronic state on the scattering is small as to be indistinguishable between the 3p and 3s states. A best fit, shown in Figure 4, is obtained for $p$=0.834 ± 0.012 while time constants are determined as $1/k_1$ = 640 fs$^{-1}$ and $1/k_2$ = 74 ps$^{-1}$. We note that we tried many schemes for the kinetics, and found that this scheme, with $k_1 \gg k_2$, produced the best fit.
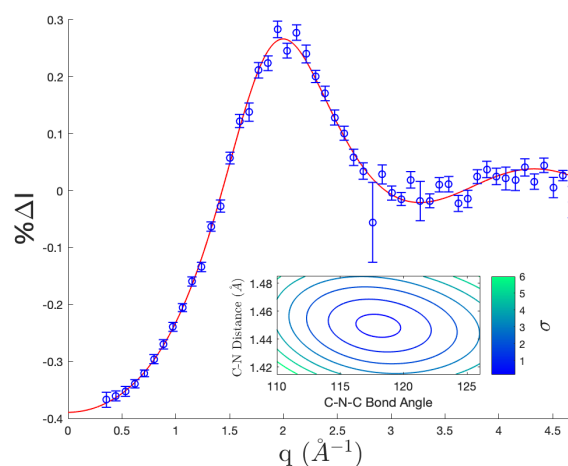


**Figure 3.** Difference scattering patterns of DMA transient as obtained from the experimental data at long time delays (blue dots) and computed using an independent atom model (red line). The red line extrapolates to -0.389 at q→0. Inset: residuals from the fit for different values of the bond length and bond angle, contour lines are at 0.2, 1, 2, 3, 4, 5, and 6 σ.

The identity of the reaction products and the bifurcation of the reaction can immediately be read out from the time dependence of the $q \to 0$ scattering signals in Figure 4. Only 83% of the molecules react in the two-step process, the overall rate of which is limited by the 74 ± 6 ps time constant. The remaining

17% of the molecules dissociate in the faster channel, with a time constant of 640 ± 130 fs. This can be seen by the kink in the curve of Figure 4, intercepted by the black dashed line, before the curve continues to decrease to -38.9% at 1 ns. This 640 fs time constant is close to the previously observed 540 fs time constant for internal conversion within the 3p manifold, suggesting that both processes have a related dynamic origin that remains to be explored. This minor channel could thus explain the high kinetic energy channel seen by Forde et al. with 193 nm excitation.
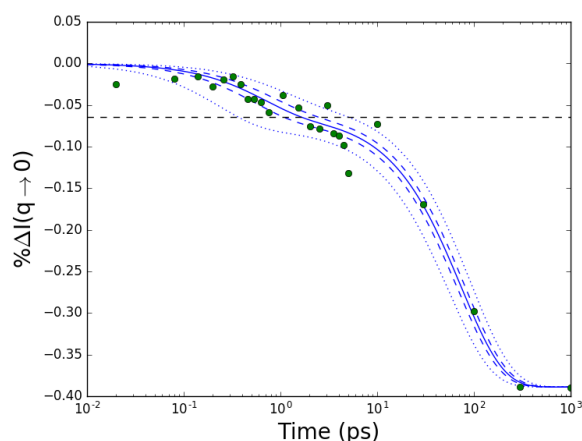


**Figure 4.** The time dependence of the decay of the TMA upon excitation at 200 nm. Plotted is the percent difference scattering signal, Eq 1, extrapolated to $q \rightarrow 0$ and scaled by the percent excitation (green dots). The fit from Eq. 6 (blue line), $1\sigma$ and $3\sigma$ tolerances (dashed and dotted blue lines, respectively) of the fit are also shown. The black dashed line is a 16.6% decrease in the $q \rightarrow 0$ scattering signal.

In summary, the X-ray scattering signal in the limit of $q \rightarrow 0$ scales as the square of the number of electrons of a molecule, a result of the coherent addition of scattering amplitudes. During a dissociation process, the coherence is lost as the fragments essentially become independent well-separated species in a random ensemble of scatterers. Consequently, the pump-probe scattering signals extrapolated to $q \rightarrow 0$ can be used to directly measure the change in the number of electrons in the molecules participating in a chemical reaction. In a dissociation reaction, the number of electrons in each fragment is different from the reactant molecule, and the quadratic dependence of the signal on the number of electrons renders the detection of this change quite sensitive. In the dissociation of TMA, we have found the changes in the $q \rightarrow 0$ scattering intensity to be in excellent agreement with the electron counts of the transient species of the reaction. Upon excitation at 200 nm, TMA decays to DMA in either the previously known relaxation to the 3s state followed by a dissociation with a 74 ps time constant; or via a faster process with a 640 fs time constant. It is possible that the latter process is directly tied to the internal conversion within the 3p manifold. In previous studies of tertiary amines, it has been noted that one of the 3p states is dissociative along the N-C coordinate.[25,26] Here we observe that in traversing the conical intersection with other 3p states along this stretch coordinate, 17% of the population dissociates, while the rest undergoes internal conversion as observed in the photoelectron spectra.[11,12] This result also highlights that X-ray scattering provides a direct measurement of populations in competing reaction channels without a reliance on knowledge of photoionization cross-sections.

The experimental scattering patterns of the transient radical DMA species is consistent with a bent structure with a bond angle of 118° and a C-N bond distance of 1.45 Å, in good agreement with computational structures. The experiment also yields scattering signals of the electronically excited TMA species. Their analysis will require an in-depth calculation of the electron density distributions and pair correlation functions, the vibrational motions of the hot reaction transients, and the coupling between electronic and nuclear motions during large amplitude vibrations.

As free-electron lasers advance into harder X-ray regimes, larger $q$-ranges can be captured, yielding even more structural detail of reaction intermediates. All of these advances will benefit from the anchor of simplicity that the coherent addition of $q \rightarrow 0$ signals provides in determining the overall chemical reaction kinetics.

### References

1  A. Barty, J. Küpper, H.N. Chapman, *Ann Rev Phys Chem* **2013,** *64,* 415-435

2  C. Bostedt, et al., *J Phys B: At Mol Opt Phys* **2013**, *46*, 164003-164023.

3  S. Boutet, G.J. Williams, *New J Phys* **2010**, *12*, 035024-035047

4  A. Moreno Carrascosa, T. Northey, A. Kirrander, *Phys. Chem. Chem. Phys.* **2017**, 19, 7853.

5  S. Ryu, R. M. Stratt, K. K. Baeck and P. M. Weber, *Journal of Physical Chemistry A* **2004***, 108*, 1189.

6  R.W. James*, The Optical Principles of the Diffraction of X-Rays*, G Bell and Sons, Ltd., London, 1948.

7  A.D. Smith, E.M. Warne, D. Bellshaw, D. A. Horke, M. Tudorovskya, E. Springate, A.J.H. Jones, C. Cacho, R.T. Chapman, A. Kirrander, R.S. Minns, *Phys Rev Lett* **2018**, *120*, 183003.

8  J.D. Cardoza, F.M. Rudakov, P.M. Weber, *J Phys Chem* **2008**, *112*, 10736-10743.

9  J.D. Cardoza, P.M. Weber, *J Chem Phys* **2007**, *127*, 036101-036102

10  N.R. Forde, M.L. Morton, S.L. Curry, S. J. Wrenn, L.J. Butler, *J Chem Phys* **1999**, *111*, 4558-4568.

11  N.R. Forde, L.J. Butler, B. Ruscic, O. Sorkhabi, F. Qi, A. Suits, *J Chem Phys* **2000**, *113*, 3088-3097.

12  E. B Warren, *X-Ray Diffraction*, Addison-Wesley, (**1969**) and Dover Publication (1990).

13  M. Ben-Nun, T. J. Martinez, P. M. Weber, and K. R. Wilson, *Chem. Phys. Lett.* **1996***,* 262, 405-414.

14  A. Kirrander, *J. Chem. Phys.* **2012**, 137, 154310.

15  T. Northey, N. Zotev, A. Kirrander, *J. Chem. Theory and Computation* **2014**, 10(11), 4911.

16  T. Northey, A. Moreno Carrascosa, S. Schäfer, A. Kirrander, *J. Chem. Phys.* **2016**, 145, 154304.

17  J. D. Geiser and P. M. Weber, *Journal of Chemical Physics* **1998**, 108, 8004.

18  M.P Minitti, J.M. Budarz, A. Kirrander, J. Robinson, T. J. Lane, D. Ratner, K. Saita, T. Northey, B. Stankus, V. Cofer-Shabica, J. Hastings and P. M. Weber, *Faraday Discuss* **2014**, *171*, 81-91;

19  J.M. Budarz, M.P. Minitti, D. V. Cofer-Shabica, B. Stankus, A. Kirrander, J.B. Hastings, P.M. Weber, *J Phys B: At Mol Opt Phys* **2016**, *49*, 034001-034012.

20  M.P. Minitti, J.M. Budarz, A. Kirrander, J.S. Robinson, D. Ratner, T.J. Lane, D. Zhu, J.M. Glownia, M. Kozina, H. T. Lemke, M. Sikorski, Y. Feng, S. Nelson, K. Saita, B. Stankus, T. Northey, J.B. Hastings & P.M. Weber, *Phys. Rev. Lett.* **2015**, *114*, 255501.

21  J. M. Glownia, et al., *Phys. Rev. Lett*.. **2016**, 117, 153003.

22  K. Gumerlock, J. Frisch, B. Hill, J. May, D. Nelson, and S. Smith, Proceedings of FEL2014, 2014, Basel, Switzerland.

23  K. H. Hellwege, A.M. Hellwege (ed.). Landolt-Bornstein: Group II: Atomic and Molecular Physics Volume 7: *Structure Data of Free Polyatomic Molecules*. Springer-Verlag. Berlin. 1976.

24  G. Herzberg, *Electronic spectra and electronic structure of polyatomic molecules*,Van Nostrand,New York, 1966

25  J.O.F. Thompson, L.B. Klein, T.I. Solling, M. J. Paterson, and D. Townsend, *Chem Sci* **2016**, 7, 1826-1839.

26  L.B. Klein, T. J. Morsing, R.A. Livingstone, D. Townsend, T.I. Solling, *Phys. Chem. Chem. Phys.* **2016**, 18, 9715-9723.